

MEASUREMENT OF THE RATE COEFFICIENT OF $\text{H} + \text{O}_2 + \text{M} \rightarrow \text{HO}_2 + \text{M}$ FOR $\text{M} = \text{Ar}$ AND N_2 AT HIGH PRESSURES

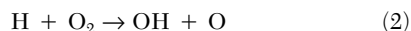
D. F. DAVIDSON, E. L. PETERSEN, M. RÖHRIG, R. K. HANSON AND C. T. BOWMAN

*High Temperature Gasdynamics Laboratory
Department of Mechanical Engineering
Stanford University, Stanford, CA 94305, USA*

OH mole fraction profiles were measured using cw UV laser absorption in shock-heated mixtures of $\text{H}_2/\text{O}_2/\text{Ar}/\text{N}_2$ between 1260 and 1375 K at 50, 68, and 115 atm. Rate coefficients for the reaction $\text{H} + \text{O}_2 + \text{M} \rightarrow \text{HO}_2 + \text{M}$, $\text{M} = \text{Ar}$ and N_2 were inferred by comparison of measured OH profiles with OH profiles modeled using the GRI-Mech v1.2 mechanism. The rate coefficient data were fit with pressure-dependent expressions that use k_∞ and F_{cent} from Cobos et al. [3]. For $\text{M} = \text{Ar}$, the measured third-order rate coefficients are consistent with a pressure-dependent expression that uses $k_0 = 7 \times 10^{17} \text{ T}^{-0.8} [\text{cm}^6/\text{mol}^2/\text{s}]$ from GRI-Mech v1.2. For $\text{M} = \text{N}_2$, the present data, when combined with the lower-temperature value of Bromly et al. [15], are consistent with a pressure-dependent expression that uses $k_0 = 2.6 \times 10^{19} \text{ T}^{-1.24} [\text{cm}^6/\text{mol}^2/\text{s}]$ over the temperature range of 700–1375 K. This expression yields k_0 values that are substantially higher than the GRI-Mech v1.2 recommendation but consistent with previous flow reactor, flame, and shock tube data and the review of Baulch et al. [24].

Introduction

The competition between the two product channels



strongly influences combustion phenomena in a wide variety of systems. Reaction (1) is an exothermic, weakly temperature-dependent, radical-terminating reaction while reaction (2) is an endothermic, strongly temperature-dependent, chain-branching reaction. The competition affects flame speeds and ignition times in the combustion of hydrogen, carbon monoxide, and hydrocarbons [1]. In nitrogen-chemistry subsystems [2], such as the conversion of fuel nitrogen to NO and in gas-phase NO_x after treatment processes, NO and NO_2 concentration profiles are sensitive to reaction (1) because of its termination role or the direct reaction of NO with HO_2 to form NO_2 .

The significant role of reactions (1) and (2) in hydrogen-oxygen systems offers the opportunity of determining the rate coefficients of both reactions in these systems. The majority of the past studies of the H_2/O_2 system has been limited to pressures of 5 atm or less, even though many practical combustion devices operate at substantially higher pressures. At very high temperatures, this limitation has not affected the predictive ability of the modeling, but at high pressures and low temperatures, in particular in the exponential growth phase of ignition in the

weak-ignition regime, modeling using only the low-pressure-limit rate coefficient for reaction (1) results in poor replication of the ignition times and radical concentration profiles. Because of the strong sensitivity of calculated ignition times and peak radical concentrations to the value of k_1 , the effect of the pressure-dependent rate coefficient falloff should be observed at pressures as low as 60 atm, even though the high-pressure limit of the rate coefficient, k_∞ , is likely not reached until pressures above 1000 atm. A discussion of the theoretical aspects of this reaction can be found in Ref. 3.

Much effort has been made to determine the rate coefficient of reaction (1); however, there is considerable scatter in the data from individual studies and substantial study-to-study variability. A review of these experiments is helpful in understanding the limitations and advantages of these studies.

Early measurements of $\text{H}_2\text{-O}_2$ ignition times by Skinner and Ringrose [4] using UV OH emission were reanalyzed by Slack [5] to determine k_1 by kinetic modeling. Emission-based ignition time measurements were also made by Just and Schmalz [6]. While ignition times in the weak and weak-to-strong ignition regime are very sensitive to the magnitude of k_1 , they are also very sensitive to impurities. Similarly, experiments that attempt to measure the rate of a relatively temperature-insensitive reaction such as (1), competing with a reaction with a large activation energy such as (2), will be sensitive to temperature.

The sensitivity to impurities can be reduced by using the method of Gutman et al. [7]. These

investigators monitored the exponential-growth phase of ignition by following the chemiluminescent emission of the reaction $\text{O} + \text{CO} \rightarrow \text{CO}_2 + \text{h}\nu$. Following a similar strategy, Skinner and co-workers [8,9] used ARAS to monitor the exponential growth of H and O atoms. The effect of small impurities on transient species profiles is to shorten the ignition time but not modify the growth constant of the species concentration profile. In these studies, the exponential growth constant rather than the ignition time was measured.

A different approach was taken by Getzinger et al. [10–12]. They noted that the approach to equilibrium in the strong-ignition case was controlled by reaction (1). They monitored this approach by following OH UV absorption or H_2O IR emission. Although this method shows good sensitivity to reaction (1), it is difficult to achieve small scatter in the measured rate because of experimental problems in determining the equilibrium values of the signals, which are needed for the calculation of the rate coefficient.

Measurements of k_1 can be extended to lower temperatures by the use of photolysis methods [13]. These investigators found that H-atom concentrations formed from photolysis in NH_3/O_2 or $\text{H}_2\text{O}/\text{O}_2$ mixtures were sensitive to k_1 . The experiments were limited to very low temperatures where H-atom removal by reaction (1) is a substantial fraction of the removal by reaction (2). When extended to higher temperatures, large scatter in the k_1 values appears.

In all the preceding experiments except those of Getzinger et al. [10–12], the region in which species profiles show the greatest sensitivity to k_1 , either in ignition time or peak concentration, is also the region where weak ignition occurs. In this region, spatial variations in the reaction progress across the shock tube diameter can occur, which may introduce scatter into the measurements.

An alternate method to determine the rate coefficient of reaction (1) is fitting species profiles in flame or flow reactor studies. This approach is exemplified by the work of Dixon-Lewis et al. [14] and Bromly et al. [15]. As we will see, these methods provide values for k_1 that are consistent with the shock tube studies.

In the present study, we take advantage of the strong sensitivity of the peak OH concentration to the magnitude of k_1 in the weak and weak-to-strong transition ignition regime for $\text{H}_2\text{-O}_2$ at high pressures. A measurement of the OH concentration profile is combined with a simple, sensitive kinetic analysis to determine the rate coefficient for the reaction $\text{H} + \text{O}_2 + \text{M} \rightarrow \text{HO}_2 + \text{M}$ in the presence of argon or nitrogen at high pressure.

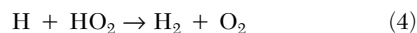
Sensitivity Studies and Design of Kinetics Experiments

The reaction mechanism describing H_2/O_2 ignition is well established [1,16]. In this study, we have

used the rate coefficient and thermodynamic data from the H/O/N subset of the GRI-Mech v1.2 mechanism (we have also renumbered the reactions). This mechanism, as published, does not include pressure dependence for k_1 . The modeling was done using the ideal-gas equation of state (EOS) kinetics solver CHEMKIN-II [17]. At the conditions of this study, the results are insignificantly different than those found using a real-gas EOS kinetics solver [18].

The modeling results can be used to identify the conditions giving good sensitivity of OH profiles to k_1 and adequate signal-to-noise ratio. We are interested in the pressure and temperature regime where, during the exponential growth phase of ignition, the reaction (1) $\text{H} + \text{O}_2 + \text{M} \rightarrow \text{HO}_2 + \text{M}$ competes strongly with the primary branching reaction (2) $\text{H} + \text{O}_2 \rightarrow \text{O} + \text{OH}$. As the temperature decreases and the pressure increases, the recombination reaction acts to delay ignition and suppress the peak radical concentration. The extent of this suppression is a function of both temperature and pressure. The region of greatest sensitivity to k_1 is easily identified in ignition time plots as occurring at temperatures below where the ignition time begins to depart and rapidly increases from the high-temperature limit expression.

A representative sensitivity of the peak OH mole fraction to the various rate coefficients is shown in Fig. 1 for 1325 K, 68 atm, and initial concentrations of 0.5% $\text{H}_2/0.25\%$ O_2/Ar . The peak OH mole fraction is most sensitive to reactions (1) and (2). In the present study, we have employed the k_2 rate expression in GRI-Mech v1.2 without change; $k_2 = 8.3 \times 10^{13} \exp(-14,413/RT)$ [$\text{cm}^3/\text{mol/s}$] [19]. Secondary sensitivity is shown to reactions



Reaction (3), the reaction with the next largest sensitivity, has a near-collisional rate coefficient at room temperature. Reaction (5), the recombination of $\text{H} + \text{OH}$ to H_2O , weakly influences the OH decay rate. Good fits to the data are achieved when the existing GRI-Mech v1.2 recommendations are used for these three secondary reactions.

Stoichiometric mixtures were used for all experiments. Leaner mixtures than stoichiometric increased the OH sensitivity to k_3 . Richer mixtures reduced the OH sensitivity to reaction (1) relative to reaction (3) and increased the sensitivity to reaction (8) $\text{OH} + \text{H}_2 \rightarrow \text{H}_2\text{O} + \text{H}$. Also, larger OH yields occurred for stoichiometric mixtures, which was important at the lowest temperatures. The H_2 mole fractions were chosen to be as small as possible and still produce usable absorption. The small H_2 mole

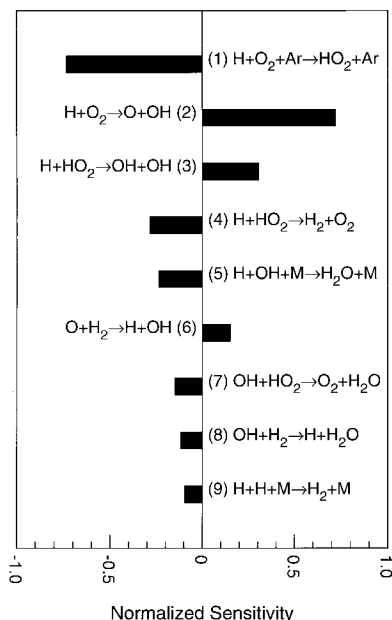


FIG. 1. Sensitivity of peak OH mole fraction to reaction rate coefficients. Normalized sensitivity is defined as $(k_i/\text{OH}_{\text{peak}}) (d\text{OH}_{\text{peak}}/dk_i)$. Initial conditions: 1325 K, 68 atm, 0.5% H_2 /0.25% O_2 /Ar.

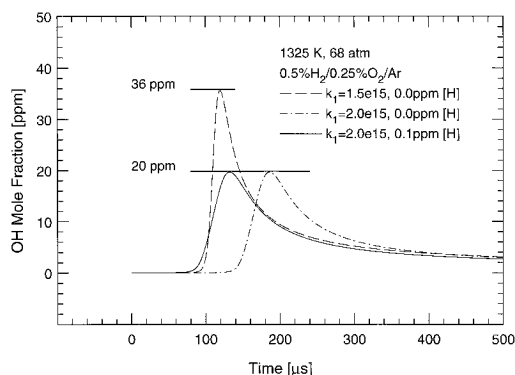


FIG. 2. Influence of impurities on the modeled OH mole fraction profiles for conditions of Fig. 1.

fractions reduced the heat release, which would have perturbed the temperature and pressure, and helped avoid the transition to detonation. In the kinetics modeling, energy release was included using the constant U and V constraint in the kinetics solver.

The reflected shock temperatures and pressures, T_5 and P_5 , for the experiments were selected such that a variation by a factor of 2 in the value for k_1 affected the peak value of OH mole fraction by a similar amount. This restricted the temperature regime of these experiments to below 1400 K. The

lower temperature limit of approximately 1250 K was set by using only data with ignition times less than 500 μs and with signal-to-noise ratios greater than about 3.

In shock tube studies, small (ppb to sub-ppm) levels of hydrogenous impurities cannot be avoided and, along with microscopic diaphragm particles that act as ignition kernels, can have a significant effect by shortening ignition time. The influence of these small impurities on the peak OH concentration and the shape of the concentration profile is generally undetectable, and this results in an advantage of the OH species profile measurements over simple ignition time measurements. Figure 2 shows the influence of added impurities on the calculated ignition time for two values of k_1 ($M = \text{Ar}$). The calculation is not significantly sensitive to the type of impurity, and we have used H atoms as a representative species. The calculated ignition times are the same for the cases of $k_1 = 1.5 \times 10^{15}$ [$\text{cm}^6/\text{mol}^2/\text{s}$] and zero H-atom impurity, and $k_1 = 2.0 \times 10^{15}$ with 0.1 ppm H atoms. Here, we are able to distinguish the different values of k_1 by the differences in the peak OH concentration, which does not change with small levels of impurities, similar in concept, at least, to the method of Gutman et al. [7].

Experimental Method

The experiments were conducted in the reflected-shock region in a stainless steel, high-purity, high-pressure shock tube. The turbo-pumped, stainless steel driven section is 5 cm diameter and 5 m long. The driver section is 7.6 cm diameter and 3 m long. Single- or double-scribed aluminum diaphragms were burst in a breech-loading system with high-pressure helium. Premixed ultrahigh purity (UHP) gases from Matheson Gases were used for the argon mixtures, and these mixtures were diluted with UHP nitrogen for the remaining mixtures.

Incident shock velocities were determined from six fast-response (1- μs) piezoelectric pressure transducers that triggered five 0.1- μs -resolution-time-interval counters. Incident shock attenuations extrapolated to the endwall were typically 3%/m. The combined temperature uncertainty resulting from the shock velocity measurement and the attenuation effects was ± 20 K. The conditions behind the reflected shocks were calculated using the one-dimensional shock relations, the Peng-Robinson real-gas equation of state, thermodynamic data from the Sandia database [17], real-gas thermodynamic correction data from Schmitt et al. [18], and assumed vibrational equilibrium and frozen chemistry [20]. The primary purpose of the real-gas frozen-shock computation was to improve the postshock temperature prediction. At 68 atm, the computed real-gas T_5 was systematically 5 K lower than the ideal-gas T_5 , while at 115 atm it was 9 K lower.

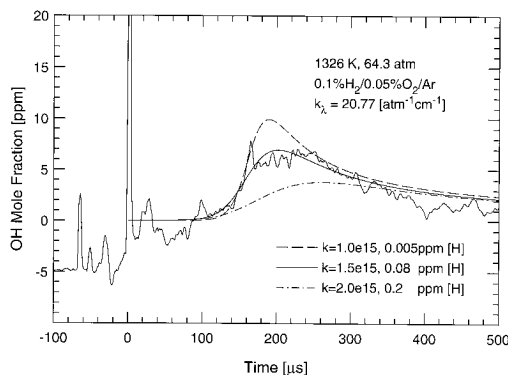


FIG. 3. Example OH mole fraction profile.

OH absorption was measured at the spectral peak at $32,629.65 \text{ cm}^{-1}$ (306.470 nm) in a simple two-beam experiment similar to that performed previously in our laboratory [21]. This wavelength corresponds to the strong OH absorption feature of the overlapping R_1 (8, 10) lines at 68 atm. At 115 atm, $32,629.50 \text{ cm}^{-1}$ (306.481 nm) was used.

Ultraviolet radiation was produced by intracavity doubling in a Spectra-Physics 380 ring-dye laser operating on Rhodamine 6G dye, which was pumped with 4 W from a Spectra-Physics Model argon-ion laser operating on all lines. The laser beam was split into a reference beam, I_0 , and a transmitted beam, I , which passed through the shock along the diameter, 20 mm from the end wall. OH concentrations were determined using the Beer–Lambert law,

$$I/I_0 = \exp(-k_\lambda P_{\text{total}} X_{\text{OH}} L)$$

where $k_\lambda [\text{atm}^{-1} \text{cm}^{-1}]$ is the high-pressure OH absorption coefficient determined previously by Davidson et al. [21] and accurate to $\pm 6\%$, $P_{\text{total}} [\text{atm}]$ is the total pressure in the reflected shock region, X_{OH} is the mole fraction of OH, and $L = 5 \text{ cm}$ is the optical path length.

An example data trace is shown in Fig. 3. The peak OH concentration at $200 \mu\text{s}$ in this figure is equivalent to 4.6% absorption. The baseline shift evident after the reflected shock beam-steering spike is a result of beam displacement on the detector when the pressure in the end section jumps from $P_1 = 3 \text{ atm}$ to $P_5 = 64 \text{ atm}$. The absence of interference emission was confirmed by noting that there was no change from the baseline signals in experiments where the laser beam was blocked intentionally. Absorption fluctuations from weak-ignition kernels were apparent over the full range of temperatures in the argon-buffer experiment, although these fluctuations were seen only at the lowest temperatures in the 75% nitrogen/25% argon buffer experiments. This difference was likely the result of being deeper into the weak-ignition regime in argon than in

nitrogen. Images of weak-ignition kernel structure similar to that expected in the present study are reported in McMillan et al. [22].

Transient beam steering from the bifurcation structure behind reflected shocks in low-specific-heat-ratio mixtures was evident in some nitrogen-buffer shocks at approximately $20 \mu\text{s}$ after the passage of the reflected shock. In separate tests in this shock tube [23], ignition times in methane/oxygen mixtures buffered with argon or nitrogen were indistinguishable over a wide range of temperatures and pressures, and this was replicated in the modeling using GRI-Mech v1.2. We may assume from this result that the small transient flow structures in the reflected-shock regime in nitrogen-buffered experiments do not significantly affect the temperatures in the bulk of the measurement volume and that the bulk temperature and pressure conditions are correct for the measured profiles.

The rate coefficients in this study were determined in the following way. The calculated peak OH mole fraction in the argon-buffered data was matched to the experimental value by varying k_1 ; this is equivalent to a time-shift of the OH mole fraction profiles. Because of the strong sensitivity of peak OH mole fraction to k_1 , a value of k_1 could be determined within approximately $\pm 10\%$. Then, the amount of radical impurity (assumed to be H atoms and typically between 0 and 1 ppm) was varied to center the peak of the model with the data. An example fit of the data is given in Fig. 3. In the case of the nitrogen-buffered data, the present values for k_1 , $M = \text{Ar}$, were fixed and k_1 , $M = \text{N}_2$, was varied. The nitrogen-buffered data were not significantly sensitive to k_1 , $M = \text{Ar}$.

Results: $M = \text{Ar}$

Mixtures of 0.5% H_2 /0.25% O_2 /Ar and 0.1% H_2 /0.05% O_2 /Ar were used for the $M = \text{Ar}$ determination. Two groups of experiments, clustered at 68 and 115 atm, were performed. The data are shown in Table 1 and in Arrhenius form in Fig. 4. The temperature range of the present data, 1260–1376 K, is too small to evidence a temperature dependence.

The scatter in the present data is smaller than reported in previous shock tube studies. The rate coefficients at 115 atm are systematically lower than those at 68 atm, consistent with a gradual falloff in the pressure-dependent behavior. Measurements by Cobos et al. [3] of this reaction at room temperature give values of $k_\infty = 4.52 \times 10^{13} (T/300)^{0.6} [\text{cm}^3/\text{mol}/\text{s}]$ and $F_{\text{cent}}(300 \text{ K}) = 0.45$. Assuming that F_{cent} is approximately constant, these results can be combined with the low-pressure rate expression in GRI-Mech v1.2, $k_0 = 7 \times 10^{17} T^{-0.8} [\text{cm}^6/\text{mol}^2/\text{s}]$, to give a pressure-dependent expression for k_1 . A representative plot of the apparent second-order rate coefficient at 1325 K of this expression is shown in

TABLE 1
M = argon data

T_5 [K]	P_5 [atm]	$k_1/10^{15}$ [cm ⁶ /mol ² /s]	$[\text{H}]_0$ ppm	$[\text{OH}]_{\text{peak}}$ ppm
Mixture: 0.1% H ₂ /0.05% O ₂ /99.85% Ar				
1326	64.3	1.5	0.08	7
1366	69.3	1.5	0.002	10
Mixture: 0.5% H ₂ /0.25% O ₂ /99.25% Ar				
1260	57.2	2.0	0.5	10
1262	54.8	1.8	0.05	12
1279	67.4	1.7	0.04	16
1290	70.1	1.7	0.07	13
1291	68.3	1.7	0.07	10
1315	70.1	1.8	0.02	19
1327	68.2	2.0	0.1	19
1344	65.8	2.0	0.25	28
1316	118.9	1.5	0.2	2
1332	113.9	1.5	0.1	5
1376	112.0	1.5	0.2	13

Fig. 5. This description of k_1 is in agreement with the present 68- and 115-atm data, as well as with other low-pressure (1–5 atm) shock tube data. The calculated 1-atm value of the rate coefficient is in excellent agreement with the recent review of Baulch et al., $k_1(\text{Ar}) = 6.2 \times 10^{17} T^{-0.8} [\text{cm}^6/\text{mol}^2/\text{s}]$ [24].

An uncertainty analysis is given in Table 2. The primary systematic sources of error come from the uncertainty in the published value of k_3 and to a much lesser extent the values of k_2 and k_4 . The OH absorption coefficient and the reflected shock temperature are not significant contributors to the

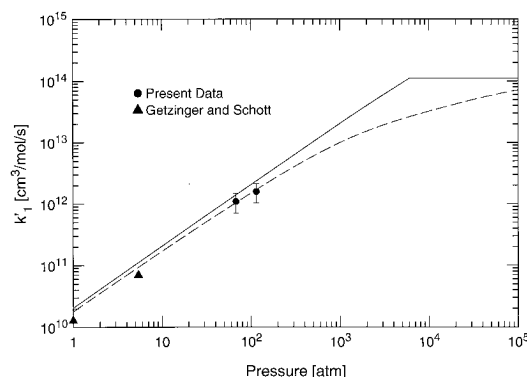


FIG. 5. Rate coefficients for the reaction $\text{H} + \text{O}_2 + \text{Ar} \rightarrow \text{HO}_2 + \text{Ar}$ at 1325 K. In this figure, k'_1 is the apparent second-order rate coefficient.

uncertainty. The random scatter of the data is mainly a result of fitting within the noise of the OH profiles.

Results: $\text{M} = \text{N}_2$

Mixtures of 0.5% H₂/0.25% O₂/24.25% Ar/75% N₂ at 50 atm were used for the $\text{M} = \text{N}_2$ determination. The data are shown in Table 3 and in Arrhenius form in Fig. 6. The scatter is again small, although the temperature variation of the present study is too small to evidence any temperature dependence.

Again using the nitrogen-partner expressions of Cobos et al. for k_∞ (identical to the value for $\text{M} = \text{Ar}$) and $F_{\text{cent}}(300 \text{ K}) = 0.50$, an improved fit for k_0 can be determined for $\text{M} = \text{N}_2$ from 1275 to 1375 K. These k_0 values can be combined with a value derived from the 700–825 K, 1-atm work of Bromley

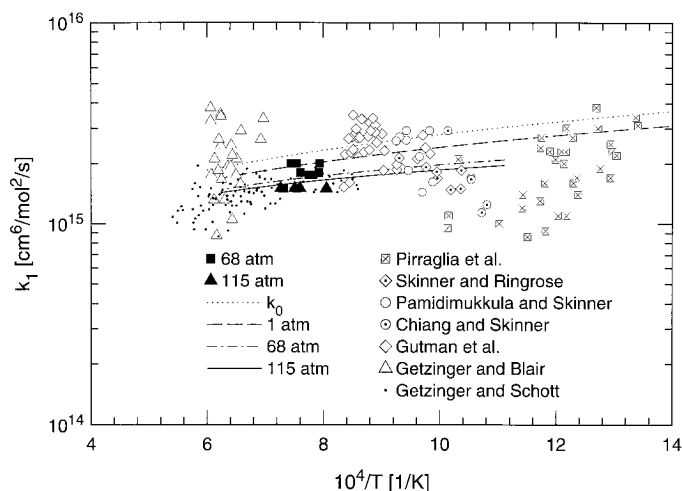


FIG. 4. Arrhenius plot of rate coefficients for the reaction $\text{H} + \text{O}_2 + \text{Ar} \rightarrow \text{HO}_2 + \text{Ar}$. Data from all references have been reevaluated using the rate expressions in GRI-Mech v1.2. The k_0 , 1, 68, and 115 atm lines were calculated using k_∞ and F_{cent} from Cobos et al. [3] and k_0 from GRI-Mech v1.2.

TABLE 2
Uncertainty analysis

Parameter	Uncertainty	Effect on k_1
Rate coefficients		
k_2	$\pm 15\%$	$\pm 15\%$
k_3	$\times 1.5$	$+32\%$
	$/1.5$	-23%
k_4	$\times 1.5$	-15%
	$/1.5$	$+13\%$
OH absorption coefficient		
k_i	$\pm 6\%$	± 2
Reflected shock temperature		
T_5	$\pm 1.5\%$	$\pm 1.5\%$
Fitting routine		
fit	$\pm 10\%$	$\pm 10\%$
Total uncertainty = $\Sigma((\Delta k_1/k_1)^2)^{0.5} = +39\%, -33\%$		

Conditions: 1275 K, 68 atm, and 0.5% H₂/0.25% O₂/Ar. Similar magnitude errors exist at 1375 K. The uncertainties in the rate coefficients k_3 and k_4 are estimated from the measurements of Keyser [25].

et al. [15] to produce a temperature-dependent $k_0 = 2.60 \times 10^{19} T^{-1.24} (+39\%, -33\%)$ [cm⁶/mol²/s] valid from 700 to 1375 K. The flow reactor work of Bromly et al. [15], the flame work of Dixon-Lewis [14], and the shock tube study of Just and Schmalz [6] are all consistent with this description of the reaction rate coefficient. The results of Slack [5] and of Getzinger and Blair [10] fall somewhat below these values. The proposed rate expression is substantially higher than the GRI-Mech v1.2

TABLE 3
M = N₂ data

T_5 [K]	P_5 [atm]	$k_1/10^{15}$ [cm ⁶ /mol ² /s]	[H] ₀ ppm	[OH] _{peak} ppm
Mixture: 0.5% H ₂ /0.25% O ₂ /24.25% Ar/75% N ₂				
1278	48.6	2.5	0.4	9
1289	54.5	2.5	0.4	8
1298	55.6	2.5	0.2	9
1304	48.8	2.7	0.1	15
1323	50.8	2.7	0.8	21
1328	52.7	2.7	0.7	17
1347	55.7	2.5	0.4	25
1350	57.2	2.7	1.0	19
1375	52.7	2.5	0.4	38

recommendation, as shown in Fig. 6. The proposed 1-atm value is approximately 30% lower and has a different temperature dependence than the Baulch et al. review [24], which recommended a value of $k_1(\text{N}_2) = 1.4 \times 10^{18} T^{-0.8}$ [cm⁶/mol²/s]. The relative collision efficiency of nitrogen to argon is $k_0(\text{N}_2)/k_0(\text{Ar}) = 37.1/T^{0.44}$. At 1500 K, this expression yields a relative collision efficiency of 1.5.

Conclusions

We present an improved method for the determination of the rate coefficient for the recombination of H + O₂ to HO₂ using narrow-linewidth laser absorption. This method is insensitive to small impurities and has a smaller scatter and uncertainty than many previous studies. This is the first effort to examine the high-temperature pressure dependence

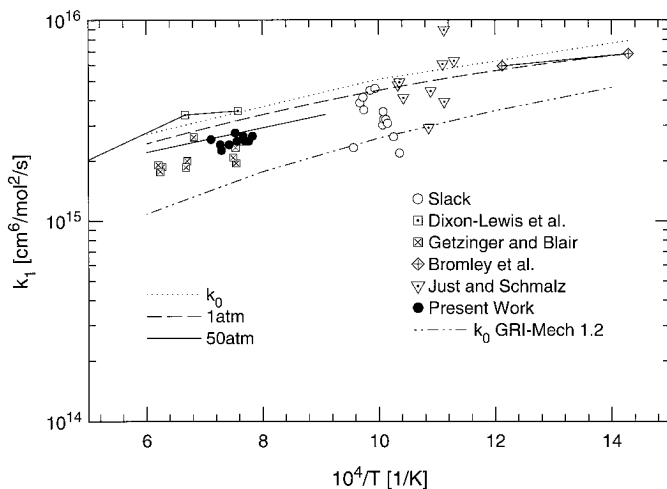


FIG. 6. Arrhenius plot of rate coefficients for the reaction $\text{H} + \text{O}_2 + \text{N}_2 \rightarrow \text{HO}_2 + \text{N}_2$. Data from all references have been reevaluated using the rate expressions in GRI-Mech v1.2. The k_0 , 1 and 50 atm lines were calculated using k_∞ and F_{cent} from Cobos et al. [5] and k_0 from the present work.

of k_1 for $\text{M} = \text{Ar}$ and N_2 . The present determination is consistent with room temperature k_∞ measurements of Cobos et al. [3] and a wide variety of shock tube, flame, and flow reactor data.

Acknowledgments

This work was supported by the Chemical Sciences Division, Office of Basic Energy Sciences, U.S. Department of Energy, with Dr. W. H. Kirchoff as contract monitor.

REFERENCES

- Warnatz, J., in *Combustion Chemistry*, (Gardiner, W. C. Jr., Ed.), Springer Verlag, New York, 1984, Chapter 5.
- Miller, J. A. and Bowman, C. T., *Prog. Energy Combust. Sci.* 15:287–338 (1989).
- Cobos, C. J., Hippler, H., and Troe, J., *J. Phys. Chem.* 89:342–349 (1985); Troe, J., *Twenty-Second Symposium (International) on Combustion*, The Combustion Institute, Pittsburgh, 1988, pp. 843–862.
- Skinner, G. B. and Ringrose, G. H., *J. Chem. Phys.* 42:2190–2192 (1965).
- Slack, M. W., *Combust. Flame* 28:241–249 (1977).
- Just, T. and Schmalz, F., AGARD Conference Proceedings No. 34, Advanced Components for Turbojet Engines, Part 2, NATO, Paris, 1968, Paper 19.
- Gutman, D., Hardwidge, E. A., Dougherty, F. A., and Lutz, R. W., *J. Chem. Phys.* 47:4400–4407 (1967).
- Pamidimukkala, K. M. and Skinner, G. B., *Proceedings of the Thirteenth Shock Tube Symposium* (Treanor, C. E. and Hall, J. G., Eds.), SUNY, Albany, 1981, pp. 585–592.
- Chiang, C. -C. and Skinner, G. B., *Proceedings of the Twelfth Shock Tube Symposium* (Lifshitz, A. and Rom, J., Eds.), Magnes Press, Jerusalem, 1980, pp. 629–639.
- Getzinger, R. W. and Blair, L. S., *Combust. Flame* 13:271–284 (1969).
- Blair, L. S. and Getzinger, R. W., *Combust. Flame* 14:5–12 (1970).
- Getzinger, R. W. and Schott, G. L., *J. Chem. Phys.* 43:3237–3247 (1965).
- Pirraglia, A. N., Michael, J. V., Sutherland, J. W., and Klemm, R. B., *J. Phys. Chem.* 93:282–291 (1989).
- Dixon-Lewis, G., Greenberg, J. B., and Goldsworthy, F. A., *Fifteenth Symposium (International) on Combustion*, The Combustion Institute, Pittsburgh, 1975, pp. 717–730.
- Bromly, J. H., Barnes, F. J., Nelson, P. F., and Haynes, B. S., *Int. J. Chem. Kinet.* 27:1165–1178 (1995).
- Frenklach, M., Wang, H., Goldenberg, M., Smith, G. P., Golden, D. M., Bowman, C. T., Hanson, R. K., Gardiner, W. C., and Lissianski, V., “GRI-Mech—An Optimized Detailed Chemical Reaction Mechanism for Methane Combustion,” Gas Research Institute Topical Report No. GRI-95/0058, 1995.
- Kee, R. J., Rupley, F. M., and Miller, J. A., “The Chemkin Thermodynamic Database,” Sandia National Laboratories Report SAND87-8215, 1987; “Chemkin-II: A Fortran Chemical Kinetics Package for the Analysis of Gas-Phase Chemical Kinetics,” SAND89-8009. UC-401, 1989.
- Schmitt, R. G., Butler, P. B., and Bergan French, N., “Chemkin Real Gas: A Fortran Package for Analysis of Thermodynamic Properties and Chemical Kinetics in Nonideal Systems,” University of Iowa Report, UIME PBB 93-006, 1994.
- Yu, C. -L., Frenklach, M., Masten, D. A., Hanson, R. K., and Bowman, C. T., *J. Phys. Chem.* 98:4770–4771 (1994).
- Davidson, D. F. and Hanson, R. K., “Real Gas Corrections in Shock Tube Studies at High Pressures,” to appear in *Israeli J. Chem.*
- Davidson, D. F., Röhrig, M., Petersen, E. L., Di Rosa, M. D., and Hanson, R. K., “Measurements of the OH A-X (0,0) 306 nm Absorption Bandhead at 60 Atm and 1735 K,” *J. Quant. Spectrosc. Radiat. Transfer* 55:755–762 (1996).
- McMillin, B. K., Lee, M. P., Paul, P. H., and Hanson, R. K., *Twenty-Third Symposium (International) on Combustion*, The Combustion Institute, Pittsburgh, 1990, pp. 1909–1914.
- Petersen, E. L., Davidson, D. F., Röhrig, M., Hanson, R. K., and Bowman, C. T., “High-Pressure Methane Oxidation behind Reflected Shock Waves,” *Twenty-Sixth Symposium (International) on Combustion*, The Combustion Institute, Pittsburgh, 1996, pp. 799–806.
- Baulch, D. L., Baulch, D. L., Cobos, C. J., Cox, R. A., Esser, C., Frank, P. Just, T., Kerr, J. A., Pilling, M. J., Troe, J., Walker, R. W., Warnatz, J., *J. Phys. Chem. Ref. Data* 21:411–734 (1992).
- Keyser, L. F., *J. Phys. Chem.* 90:2994–3003 (1986).

COMMENTS

J. V. Michael, Argonne National Laboratory, USA. You have determined values for both k_0 and k_∞ using only your high temperature data. Have you considered extending your calculations down to lower temperatures in order to see how you agree with the values of Hsu et al. [1]?

REFERENCE

1. Hsu, K.-J., Anderson, S. M., Durant, J. L., and Kaufman, F., *J. Phys. Chem.* 93:1018 (1989).

Author's Reply. Though not discussed in this paper, our extrapolated values of k_0 for the reaction $\text{H} + \text{O}_2 + \text{N}_2 = \text{HO}_2 + \text{N}_2$ are in very good agreement with the measurements of Hsu et al. [1] which were obtained for pressures less than 50 torr. At 298 K, we are above their value by 3%; at 433 K, we are above by 14%; and at the upper temperature limit of their work 639 K we are above by 40%. This is clearly within their uncertainty alone except at the highest temperature.

•

William R. Anderson, U.S. Army Research Laboratory, USA. The authors mention an inability to achieve reliable measurements of this rate coefficient at the high pressure limit. I noted the measurements were all performed at at least moderately high temperatures, presumably in order to achieve high enough radical concentrations to make the measurements feasible. If the apparatus were modified to make photolysis of radical precursors possible (a laser photolysis- or flash photolysis-shock tube approach), a significant amount of radicals could be introduced at lower temperatures (where, as we all know, the high pressure limit

rate coefficient is observed at lower pressures). Could this make measurements of the high pressure limit rate coefficient feasible?

Author's Reply. Low-pressure, low-temperature shock tube photolysis experiments were performed by Pirraglia et al. (Ref. 13 in the paper), but do not lend themselves to extension to higher pressures. Even at low temperatures very high pressures are still needed to approach the high-pressure limit. For example: for the rate coefficient k_1 , at 800 K and 200 atm, the reduced pressure, P_r , is only 0.12. This is still too low for a useful measurement of the high-pressure limit.

•

William J. Pitz, Lawrence Livermore Laboratories, USA. You stated that $\text{H} + \text{O}_2 + \text{N}_2 \rightleftharpoons \text{HO}_2 + \text{N}_2$ is in the low pressure limit up to 10,000 ATM. This would give the impression that modelers using detailed chemical kinetics need not worry about fall-off behavior for $\text{H} + \text{O}_2(+\text{N}) = \text{HO}_2(+\text{N})$ for most pressures encountered in combustion, including those found in super-critical water oxidation. However, the most important third body collider is water which gives much more stabilization than N_2 . I would recommend caution in implying that one needs not to worry about fall-off of $\text{H} + \text{O}_2(+\text{N}) = \text{HO}_2(+\text{N})$ in combustion devices.

Author's Reply. At lower temperatures, that is nearer to 300 K than 1200 K, the fall-off behavior of this reaction can become very important and should always be included in calculations. We also agree about the importance of the reaction for $\text{M} = \text{H}_2\text{O}$ and plan to measure the rate coefficient with this collision partner in the near future.